

Theory of selective adsorption for He-LiF: Azimuthal and polar dependent intensities

N. Garcia,* V. Celli, and Frank O. Goodman†

Department of Physics, University of Virginia, Charlottesville, Virginia 22901

(Received 5 June 1978; revised manuscript received 21 August 1978)

An exact, nonperturbative calculation of the specular and diffracted intensities for He on LiF (001) accounts for all the features seen in the most recent experiments in the selective adsorption region for azimuthal and polar dependence. It is observed from the computed intensities that all of the family of beams having the same G_y lead to the same shape of the resonant structure. In particular, the (0,0), (1,0), and (2,0) beams present minima in the azimuthal dependence and maxima in the polar one, while the (1,1) and (2,1) present the opposite shape. This behavior seems to be general, and applicable to other systems.

I. INTRODUCTION

In the last few years the technique of atomic-beam scattering has been proved to be efficient and applicable to many kinds of surfaces.¹ Diffracted intensity patterns and detailed studies of resonances with surface-bound states provide a large amount of information on the gas-solid interaction potential and on the surface topography. The interpretation of the experimental diffraction patterns for He-LiF(001) at incident energies of 60 meV ($k_i \approx 11 \text{ \AA}^{-1}$) (Ref. 2) has been successfully accomplished using the hard corrugated surface (HCS) model,³⁻⁵ although this model does not include the attractive part of the potential that gives a well approximately 8 meV deep. The experimental data are not much affected by the attractive well for incidence angles $\theta_i < 50^\circ$, thus explaining the success of the HCS model in this range; for $\theta_i > 50^\circ$, however, the presence of bound-state resonances is obvious but no detailed theoretical fit has been attempted, due also to some uncertainty in the data.

On the other hand, the existing data for lower incident energy ($k_i \approx 6 \text{ \AA}^{-1}$) show clearly a resonance pattern in the intensity curves versus polar or azimuthal incident angle. It is then evident that the introduction of an attractive long-range well is necessary in the theory to explain the experiments in detail. The available experimental evidence⁶⁻⁹ confirms the theoretical prediction that the attractive potential should fall off as z^{-3} at large enough distances z from the surface, due to the polarization forces between the He atom and the crystal.¹⁰ Also, a comparative fit of the bound states by different kinds of potentials indicates the above-mentioned asymptotic behavior.¹¹

This paper is concerned with the analysis of very recent experimental data^{8,9} on He-LiF(001) at low incident energy ($k_i \approx 6 \text{ \AA}^{-1}$), which were taken for every 0.33° of the incident angle. In it, we pre-

sent the Rayleigh approach to the exact quantum-mechanical theory of the scattering of atoms from a hard corrugated surface plus an attractive well (HCSW), which was developed recently.¹² This theory has been applied successfully¹² to the scattering from stepped surfaces represented by a one-dimensional corrugation, but is harder to use for two-dimensional corrugations. Fortunately, the corrugations involved in alkali halides (and in most all perfect plane surfaces) seem to fall within the range of applicability of the Rayleigh method as a practical procedure. The use of the Rayleigh approach for the HCSW model with the long-range attractive part was first developed by Harvie and Weare¹³ and applied by them to some of the data that are the subject of this study; our method, however, differs in some important aspects and our calculations are compared with the entire body of available data.

The paper is organized as follows: in Sec. II we introduce the general theory and develop it in particular for a potential with a z^{-3} long-range part; in Sec. III we present the result of computations for the He-LiF(100) system and compare with experiment; in Sec. IV we draw conclusions and discuss the insight gained by this work.

II. MODEL POTENTIAL AND THE RAYLEIGH APPROACH

The exact quantum-mechanical theory for the HCSW model has been presented in Ref. 12, for a general potential of the form

$$V(\vec{r}) = \infty \quad \text{for } z < \zeta(\vec{R}), \quad (1a)$$

$$V(\vec{r}) = V(z) \quad \text{for } z > \zeta(\vec{R}), \quad (1b)$$

where $\vec{r} = (\vec{R}, z)$, z is the coordinate perpendicular to the surface, and $\zeta(\vec{R})$ is the surface corrugation profile. In particular, the attractive part of the potential, $V(z)$, is approximated by

$$V(z) = -D \text{ for } z < \beta, \quad (2a)$$

$$V(z) = -D \left(\frac{\alpha + \beta}{\alpha + z} \right)^3 \text{ for } z > \beta, \quad (2b)$$

where D , α , β are parameters to be fixed by fitting to the observed bound states. Using this potential it has been possible to fit all the known bound states for all the systems that have been presented in the literature with less than 4% maximum deviation from the experiments.

The integral equation for the sources of the reflected field on the hard wall $z = \zeta(\vec{R})$ is, following Garcia, Goodman, Celli, and Hill,¹²

$$\psi_i(\vec{R}, \zeta(\vec{R})) = \int_A s(\vec{R}') \sum_{\vec{G}} \exp[i(\vec{K} + \vec{G}) \cdot (\vec{R} - \vec{R}')] \times g_{\vec{G}}(\zeta(\vec{R}), \zeta(\vec{R}')) d^2\vec{R}', \quad (3)$$

where A is the area of the surface unit cell, \vec{G} are the reciprocal-lattice vectors, \vec{K} is the parallel momentum of the incident atom, $\vec{k}_i = (\vec{K}, k_z)$, and $\psi_i(\vec{R}, z)$ is the incident wave function as modified by the presence of the attractive potential $V(z)$. Finally, $g_{\vec{G}}(z, z')$ is the one-dimensional Green's function in the presence of the potential $V(z)$ with a parallel momentum transfer \vec{G} . For the $V(z)$ given by (2), the value of $g_{\vec{G}}$ in the region where it is needed is as follows:

Case (i) $z < \beta$ and $z' < \beta$:

$$g_{\vec{G}}(z, z') = (i/k_{\vec{G}z}') \{ \exp(ik_{\vec{G}z}'|z - z'|) + R(k_{\vec{G}z}') \exp[-ik_{\vec{G}z}'(z + z')] \}. \quad (4)$$

Case (ii) $z \rightarrow \infty$ and $z' < \beta$:

$$g_{\vec{G}}(z, z') = i \left(\frac{1 - |R(k_{\vec{G}z}')|^2}{k_{\vec{G}z} k_{\vec{G}z}'} \right)^{1/2} \times \exp[i(k_{\vec{G}z} z - k_{\vec{G}z}' z' + \phi)], \quad (5)$$

where $k_{\vec{G}z}$ are the perpendicular components of the diffracted wave vectors: $k_{\vec{G}z}^2 = k_i^2 - (\vec{K} + \vec{G})^2$; $k_{\vec{G}z}'$ are the energy-shifted values of $k_{\vec{G}z}$ due to the well depth D : $k_{\vec{G}z}'^2 = k_{\vec{G}z}^2 + 2MD/\hbar^2$, where M is the gas atom mass; $R(k_{\vec{G}z}')$ are reflection coefficients for a plane wave incident on $V(z)$ from the region $z < \beta$; and ϕ is a phase angle that will not be needed.

The solution of integral equation (5) for a two-dimensional corrugation requires a considerable amount of computer time. The task is very much simplified if it is permissible to substitute $(z - z')$ for $|z - z'|$ in the expression (4) for the Green's function. This is what we call the *Rayleigh approach for the HCSW model*. The corresponding replacement for the HCS model and the equivalence to the conventional Rayleigh method has been dis-

cussed by Garcia and Cabrera¹⁴; an alternative approach is the use of the extinction theorem which has been discussed recently by Marvin and Toigo for a wide class of HCSW models.¹⁵

With the Rayleigh assumption, Eq. (3) can be written

$$\psi_i(\vec{R}, \zeta(\vec{R})) = \sum_{\vec{G}} B_{\vec{G}} \exp[i(\vec{K} + \vec{G}) \cdot \vec{R}] \times \{ \exp[ik_{\vec{G}z}' \zeta(\vec{R})] + R(k_{\vec{G}z}') \exp[-ik_{\vec{G}z}' \zeta(\vec{R})] \}, \quad (6)$$

with

$$B_{\vec{G}} = \frac{i}{k_{\vec{G}z}'} \int_A s(\vec{R}) \exp[-i(\vec{K} + \vec{G}) \cdot \vec{R}'] \times \exp[-ik_{\vec{G}z}' \zeta(\vec{R}')] [1 + R(k_{\vec{G}z}')] d^2\vec{R}'. \quad (7)$$

Now the expression for the scattering amplitude $A_{\vec{G}}$ is

$$e^{-i\phi} A_{\vec{G}} = i \left(\frac{1 - |R(k_{\vec{G}z}')|^2}{k_{\vec{G}z} k_{\vec{G}z}'} \right)^{1/2} \times \int_A s(\vec{R}) \exp[-i(\vec{K} + \vec{G}) \cdot \vec{R}] \times \exp[-ik_{\vec{G}z}' \zeta(\vec{R})] d^2\vec{R} - R^*(k_{\vec{G}z}') \delta_{\vec{G}, \vec{0}}, \quad (8)$$

but from Eqs. (7) and (8) we obtain a straightforward relation between $B_{\vec{G}}$ and $A_{\vec{G}}$

$$e^{-i\phi} A_{\vec{G}} = \left(\frac{k_{\vec{G}z}'}{k_{\vec{G}z}} \right)^{1/2} \frac{[1 - |R(k_{\vec{G}z}')|^2]^{1/2}}{1 + R(k_{\vec{G}z}')} B_{\vec{G}} - R^*(k_{\vec{G}z}') \delta_{\vec{G}, \vec{0}}. \quad (9)$$

This completes the relation between the diffraction intensities

$$P_{\vec{G}} = (k_{\vec{G}z}/k_{\vec{G}z}') |A_{\vec{G}}|^2 \quad (10)$$

and the coefficients $B_{\vec{G}}$.

The following points should be noted: (i) Equation (6) reduces exactly to the HCS model (no attractive well included) when $R(k_{\vec{G}z}') = 0$. (ii) It must be stressed again that $\psi_i(\vec{R}, z)$ is the incident wave function in the presence of the attractive potential $V(z)$ and that for $z < \beta$

$$\psi_i(\vec{R}, z) = \left(\frac{1 - |R(k_{\vec{G}z}')|^2}{k_{\vec{G}z} k_{\vec{G}z}'} \right)^{1/2} \exp(-ik_{\vec{G}z}' z) \times \exp(-i\vec{K} \cdot \vec{R}). \quad (11)$$

(iii) Once the reflection coefficients $R(k_{\vec{G}z}')$ are found [by numerical integration of the one-dimensional Schrödinger equation for $V(z)$], Eq. (7) is solved numerically on a discrete set of points \vec{R} for the coefficients $B_{\vec{G}}$, which completely solve the problem through (9) and (10). This GR

numerical procedure is cheaper and easier to apply than the RR procedure of solving (6) and (7) for $s(\bar{R})$.¹⁴ (iv) The last term in (8) and (9) corresponds to the specular reflected wave in the potential $V(z)$. Such a term is present even though $V(z)$ is purely attractive. (v) The range of validity of the Rayleigh approach is the same here as in the HCS model.¹⁶ For the He-LiF(100) system the approach is not strictly valid, but the strength of the corrugation is close enough to the limit of analytic validity that one obtains in practice a useful result for the incident energy of interest here ($k_i = 6 \text{ \AA}^{-1}$). For instance, for the profile defined in Eq. (13) below, the range of strict validity of the Rayleigh method for $\zeta_2 = 0$, according to Ref. 16, is limited by $G_0 \zeta_1 = 0.592$, corresponding to $\zeta_1 = 0.265 \text{ \AA}$. The reason why the method works at small k_i values is, apparently, that the lack of convergence manifests itself in the large $k_{\bar{z}}$ components.

III. RESULTS FOR He-LiF(001)

The experimental data of primary interest to us here are those taken by Frankl and co-workers^{8,9} at a surface temperature of 125 K, where inelastic effects are expected to be relatively unimportant, as shown by the fact that the Debye-Waller factor is of the order of 0.5. A careful and detailed experimental study of the same He-LiF(100) system at low temperature had been done previously by Boato *et al.*,² for an incident wave vector $k_i \approx 11 \text{ \AA}^{-1}$. Most of these earlier data could be explained theoretically on the basis of the HCS model without a well,³⁻⁵ while the resonances could be understood qualitatively in terms of a simple square well.¹⁷ Subsequent studies by Chow and Thompson¹⁸ did much to clarify the nature of the resonant structure and to show that an elastic scattering theory is sufficient to account well for the low-temperature observations. Their predictions of the splittings of resonances with two degenerate surface bands are well borne out by experiments and confirmed by more detailed calculations of the entire surface bound state band structure for He on LiF(100).¹⁹ Finally, calculations for the HCSW model with a long-range potential, showing agreement with the data of Frankl and co-workers^{8,9} have been reported by Harvie and Wear¹³ for the azimuthal dependence of the specular beam. The detailed agreement of these calculations with experiment is remarkable, but it must be stressed that all comparisons have been done for the specular beam only, that is to say without considering the other 16 diffracted beams that appear in the He-LiF(100) scattering experiments⁹

for $k_i = 5.76 \text{ \AA}^{-1}$.

We give here the results of a complete calculation for all the diffracted beams and a detailed comparison with the data of Ref. 9, which are the most accurate available. These data are reproduced as the lower graphs in Figs. 1 and 2.

The calculations were performed using the model described by Eqs. (1) and (2) with $D = 8.0 \text{ meV}$, $\alpha = 1.41 \text{ \AA}^{-1}$, and $\beta = 1.04 \text{ \AA}^{-1}$. The bound-state energies for this potential $V(z)$ are $\epsilon_n = -6.05, -2.50, -0.80, -0.19, \text{ and } -0.04 \text{ meV}$ for $n = 0, 1, 2, 3, \text{ and } 4$, in good agreement with the values inferred directly from the positions of the resonances⁹ and with those used in other calculations.¹³ The corrugation used is of the

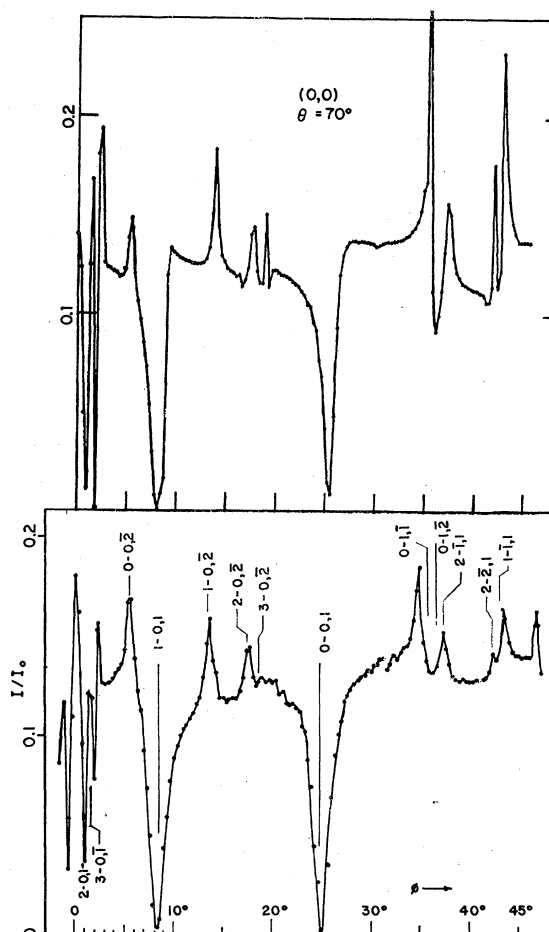


FIG. 1. Theory (above) and experiments Ref. (9) (below) for azimuthal (ϕ_i) dependence of the specular intensity at $\theta_i = 70^\circ$. The theoretical plot gives the elastic intensity multiplied by a factor of 0.43, accounting for the Debye-Waller factor and other possible corrections. Straight line segments join points determined at $\Delta\phi_i = 0.3^\circ$ in the theory and 0.333° in the experiment.

type

$$\zeta(\vec{R}) = \frac{1}{2}\zeta_1[\cos(2\pi x/a) + \cos(2\pi y/a)] + \zeta_2 \cos(2\pi x/a) \cos(2\pi y/a) \quad (12)$$

for different values of the parameters ζ_1 and ζ_2 and for a unit cell size $a = 2.817 \text{ \AA}$, consistent with the observed value $G_0 = 2.23 \text{ \AA}^{-1}$ of the basic reciprocal lattice vector.

In Figs. 1 and 2 we present the calculated specular intensities (upper plots) as a function of the azimuthal angle ϕ_i and of the polar angle Θ_i , respectively for the corrugation parameters $\zeta_1 = 0.307 \text{ \AA}$, $\zeta_2 = 0.017 \text{ \AA}$.²⁰ The experimental data

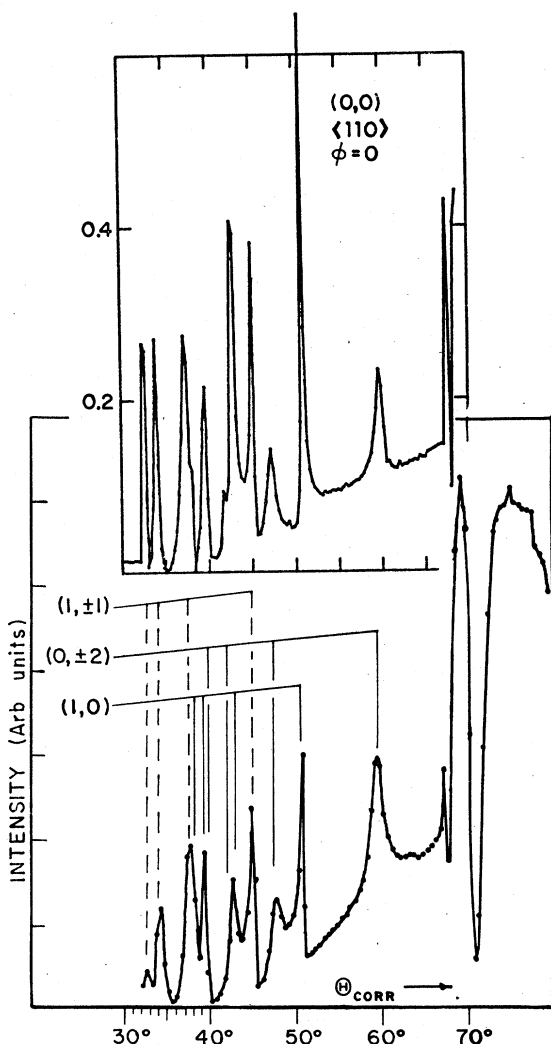


FIG. 2. Theory (above) and experiment (below) for the polar angle (Θ_i) dependence of the specular intensity at $\phi_i = 0^\circ$. The theoretical plot is multiplied by a factor of $\exp(-0.37 \cos^2 \Theta_i)$ as obtained experimentally Ref. (2) and is drawn as in Fig. 1, with $\Delta\Theta_i = 0.3^\circ$; experimentally $\Delta\Theta_i = 0.5^\circ$.

are shown in the lower graphs of the same figures; we have chosen not to superimpose theory and experiment, as done in Ref. 13, so that the graphs do not cover each other and the fine structure can be appreciated. All the observed structure is clearly reflected in the calculations and in addition some computed resonance features are more evident than in the data, as for example the $(3 - 0, \bar{2})$ and the $(2 - \bar{2}, 1)$ peaks in Fig. 1. It is possible that the experimental structure is smeared out by inelastic effects, but it may well be that the experimental data are not completely resolved, and neither is the theory for $\Delta\Theta_i = \Delta\phi_i = 0.3^\circ$, which are the intervals used in the plots.

As another example, we note that in Fig. 2 there is a hint of fine structure at $\Theta_i = 38^\circ$ on the right-hand shoulder of the peak at 37.5° , in correspondence with the expected position of the $(3 - 1, 0)$ resonance, which should be very narrow because it comes from the highest observed level. Similar remarks apply to the $(2 - 0, \pm 2)$ resonance at 41.5° . We have resolved these peaks with $\Delta\Theta_i = 0.05^\circ$ and are then able to see the expected fine structure, as shown in Fig. 3. We conclude from these calculations, and from similar studies that we have carried out for He on graphite, that there are, in the elastic theory, resonances with a very narrow width, well below the present experimental resolution. We conclude that, up to an angular resolution of 0.3° , the elastic theory and the experiments agree well for the specular peak.

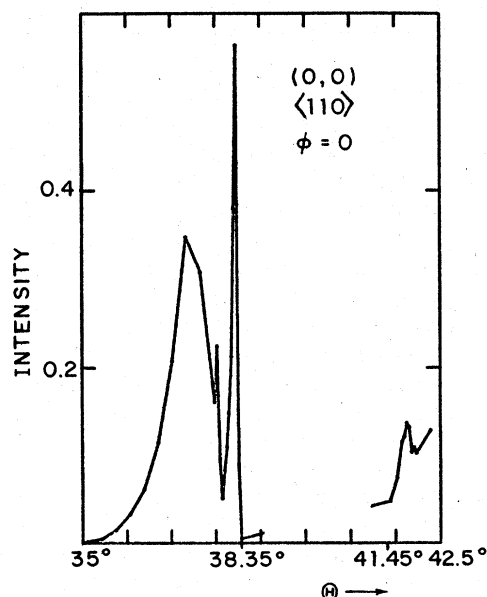


FIG. 3. Fine-scale details of the theoretical plot in Fig. 2, with $\Delta\Theta_i = 0.05^\circ$. Observe the new structure appearing, which is unresolved in the experiments.

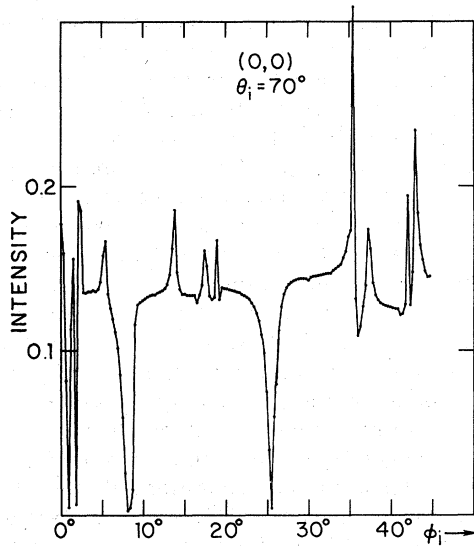


FIG. 4. Replica of the theoretical plot in Fig. 1 (azimuthal dependence of the specular intensity at $\Theta_i=70^\circ$), but with the second harmonic of the surface corrugation profile ζ_2 set to zero.

We turn now to a description of the theoretical predictions for the diffracted beams, which have not yet been studied in detail experimentally. The calculations were performed for two values of the second harmonic in the surface corrugation, $\zeta_2 = 0$ and 0.017 \AA . Figures 4–8 are azimuthal plots for $\Theta_i = 70^\circ$. Figure 4 gives the $(0, 0)$ beam for $\zeta_2 = 0$ and should be compared with the analogous

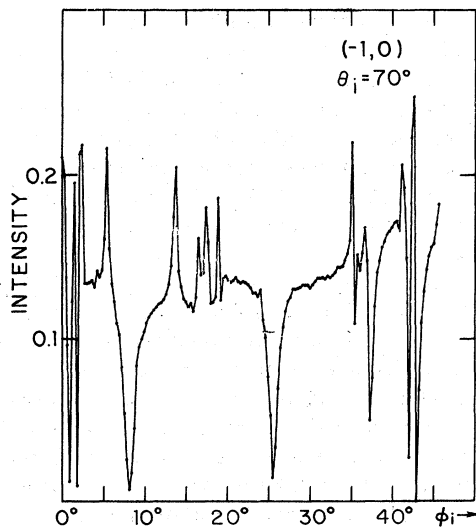


FIG. 5. Computed azimuthal dependence of the $(\bar{1}, 0)$ beam at $\Theta_i=70^\circ$. The surface profile is the same as in the theoretical plot of Fig. 1, but no correction factor is applied here.

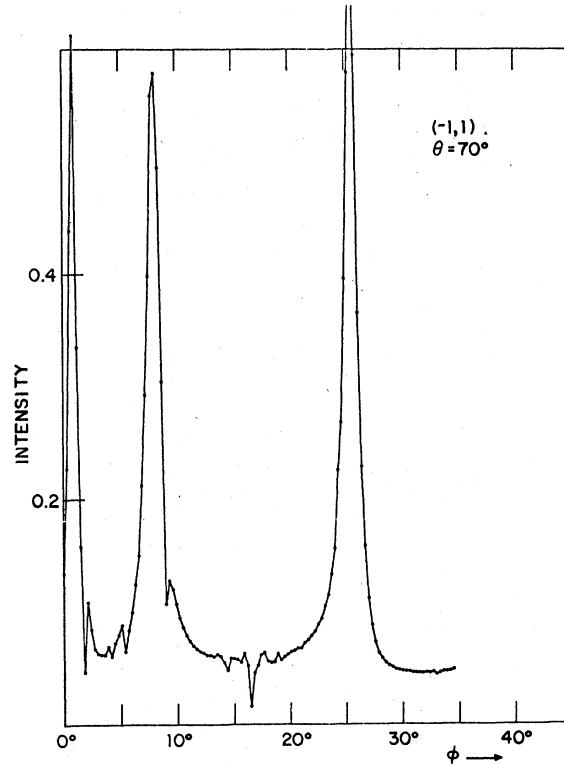


FIG. 6. Same plot as Fig. 5 for the $(\bar{1}, 1)$ beam. Note that the minima in the two previous figures are maxima here.

plot for $\zeta_2 = 0.017 \text{ \AA}$ in the upper part of Fig. 1. We observe that there is perhaps a better agreement with experiment for ϕ near 13° when the second harmonic is not included but the structure near 43° is reproduced better with the second

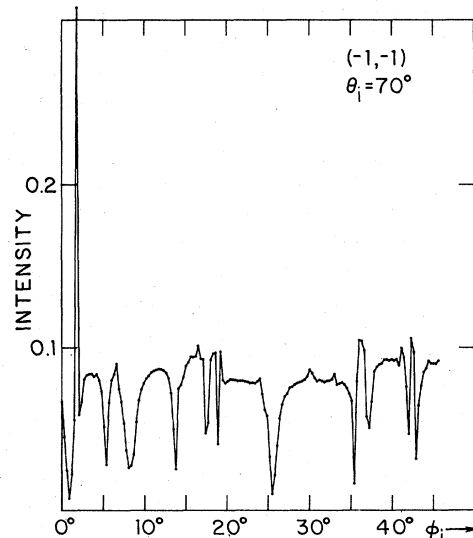


FIG. 7. Same plot as Fig. 5 for $(\bar{1}, \bar{1})$ beam.

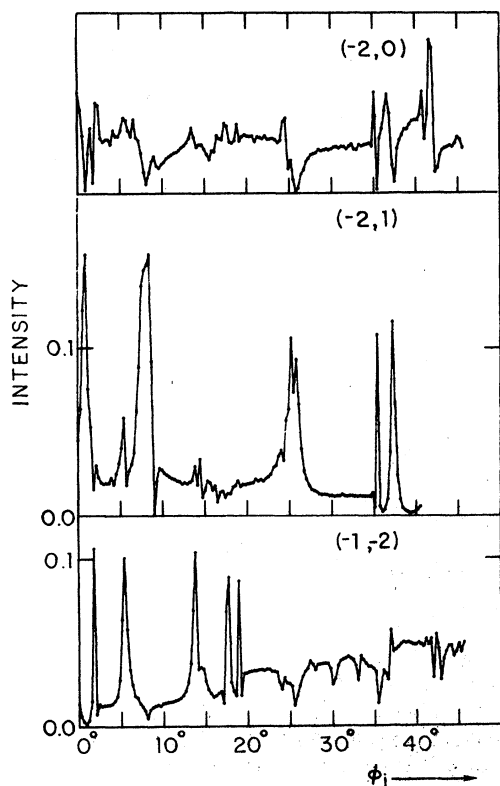


FIG. 8. Same as in Fig. 5 for $(\bar{2}, 0)$, $(\bar{2}, 1)$, $(\bar{1}, \bar{2})$. Note the similarity of $(\bar{2}, 0)$ with Figs. 4 and 5 and of $(\bar{2}, 1)$ with Fig. 6.

harmonic. To resolve this point one should re-examine the fit to the data at $k_i = 11 \text{ \AA}^{-1}$ with the attractive well included. For all the other beams, we see practically no difference due to the second harmonic in the surface corrugation and we reproduce here only the results for $\zeta_2 = 0.017 \text{ \AA}$. Figure 5 gives the $(\bar{1}, 0)$ beam, which is seen to be nearly the same as the $(0, 0)$. On the other hand, the behavior of the $(\bar{1}, 1)$ beam, shown in Fig. 6, is almost the opposite: the large minima in $(0, 0)$ and $(\bar{1}, 0)$ correspond to large maxima in $(\bar{1}, 1)$. This is in agreement with previous calculations by Chow and Thompson^{17,18} and Garcia.¹⁷ The $(\bar{1}, \bar{1})$ beam, however, is intermediate between those discussed above, as shown in Fig. 7. The family of beams $(\bar{2}, 0)$, $(\bar{2}, 1)$, and $(\bar{1}, \bar{2})$ is displayed in Fig. 8. We observe that $(\bar{2}, 0)$ looks like a small scale replica of the specular beam. In this case, the similarity persists even where the $(\bar{1}, 0)$ beam departs from the $(0, 0)$. Analogously, $(\bar{2}, 1)$ is a faithful copy of $(\bar{1}, 1)$, with maxima where minima appear in the specular. No overall similarities are observed in the $(\bar{1}, \bar{2})$ beam.

The following remarks are important at this

point: (i) The elastic theory seems to show quite definitely that all the beams with the same G_y have the same azimuthal structure. In our case, the $G_y = 0$ beams $(0, 0)$, $(\bar{1}, 0)$, and $(\bar{2}, 0)$ give very similar plots, as do $(\bar{1}, 1)$ and $(\bar{2}, 1)$, both of which have $G_y = 2\pi/a$. (ii) There is some experimental evidence to support this conclusion, even in cases where inelastic effects are probably important. In particular, there are data by the Erlangen group in which minima are found in all the reported $G_y = 0$ beams for the $(3 - \bar{1}, 0)$ resonance in H-KCl(001).²¹ In He-NaF(001), which is closer to the system we consider, Liva and Frankl²² noted that the $(\bar{1}, 1)$ and $(\bar{2}, 1)$ beams present the same behavior, with maxima at resonance, whereas $(\bar{1}, 0)$ and $(\bar{2}, 0)$ have minima, as the specular does, for transitions via the $(0, 1)$ vector that occur near $\Theta_i = 70^\circ$ and $\phi_i = 0$. While a complete comparison of theory and experiment is still to be done with a HCW and a realistic attractive well, model calculations for this system by Chow and Thompson¹⁸ show agreement with the behavior mentioned by Wood *et al.*²³ for the $(\bar{1}, \bar{1})$ and $(1, 2)$ beams. (iii) The behavior and trends observed here for different beams seem to be quite general. Liva and Frankl²² have noted that the proximity of the diffracted beam to resonance produces maxima, but we have found that maxima appear also in beams which are not neighbors of the resonant beam, as in the case of $(\bar{1}, 1)$ and $(\bar{1}, 2)$. (iv) Obviously a more extended set of co-ordinated experiments would be necessary to confirm the statement made in (i) and to elucidate the role of inelastic processes, if any.

We have also computed the polar angle dependence of the diffracted beams for $30^\circ < \Theta_i < 70^\circ$ at $\phi_i = 0$ (Fig. 9). We observe the same correlations as in the azimuthal plots: the $(0, 0)$ and $(\bar{1}, 0)$ beams are similar, while the $(\bar{1}, 1)$ beam has minima where the others have maxima.

All the beams not presented in the figures (there are 16 diffracted beams for most angles) have small intensities and do not seem very relevant.

All the sharp features seen in these calculations can be "accounted" in terms of bound state resonances. We stress this point because in the case of scattering from a stepped-surface potential, built to model He-Cu(117), we have noted a structure 0.05° narrow corresponding to the threshold condition for scattering into an intermediate state at the bottom of the attractive well.¹² It is possible that this effect is not seen in the present calculation because the effective corrugation is smaller than for a stepped surface. For the flat-bottom potential that we are using the threshold condition is $k_{\bar{z}}' = 0$ for some \bar{G} , and it is easy to see from

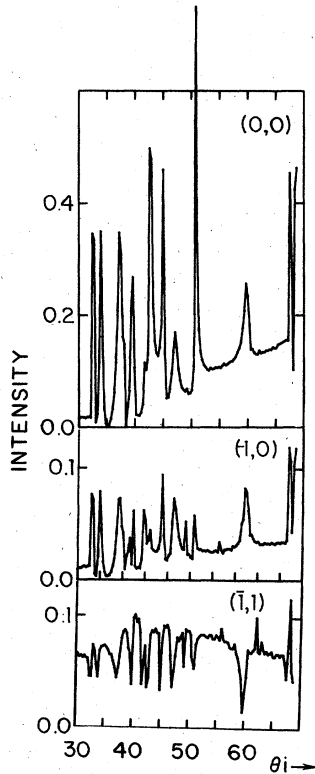


FIG. 9. Computed plots of the polar dependence for $\phi_i=0$ of the $(0,0)$, $(\bar{1},0)$, and $(\bar{1},1)$ beams. These are drawn as the upper plot in Fig. 2, but without a Debye-Waller factor. In this case, too, $(0,0)$ and $(\bar{1},0)$ have the same behavior; one is practically the copy of the other as in Figs. 4, 5, and 8. On the other hand, $(\bar{1},1)$ has the opposite behavior, as happens for the $(\bar{1},1)$ and $(\bar{2},1)$ beams in azimuthal dependence.

the formulas of Sec. II and the expression for $R(k_{G_x}')$ that an analytic singularity in the scattering amplitude must be present when k_{G_x}' goes from real to imaginary.

For a more general well with a rounded bottom an analytic singularity should still be present, but it is probably weaker than in the case of a flat bottom. We plan to study this question in more detail, because the bottom threshold effect, *if observable experimentally*, would provide a direct way to determine one of the well parameters. The effect can be looked for by the same techniques that are used for bound-state resonances, since the kinematic conditions are of the same type, namely, $k_i^2 = (\vec{K} + \vec{G})^2 + 2mD/\hbar^2$. However, it is probably necessary to obtain experimentally a derivative plot in order to bring out clearly the analytic singularity.

IV. CONCLUSIONS

(i) The specular intensity reported experimentally⁹ can be explained with the HCSW model¹³ by incorporating a long-range z^{-3} potential. It turns out that the position of the resonances in the $V(z)$ potential and the shape of the corrugation are sufficient to describe the whole observed structure.

(ii) The behavior at resonance seems to be the same for beams having the same G_y component, as for example the $(\bar{m},0)$ and $(\bar{m},\bar{1})$ families in our case. This observation is in agreement with all previous experiments²¹⁻²³ and calculations,^{17,18} but of course the experimental confirmation is in few cases.

(iii) It is evident that an experimental check of the above prediction is necessary for three reasons: (a) because the resonant structure is more clear in some diffracted beams than in the specular; (b) because one wants to know if all diffraction follows an elastic behavior and thus the absorption of gas is not important in these non-equilibrium experiments; and (c) because general inferences about the surface potential and further simplifications in the theory may be possible, through a separation of x and y coordinates, if the trends described here for the different beams are indeed observed.

(iv) Phonons seem to be unimportant in the scattering under resonant conditions. We do not understand this. In fact, very recent time-of-flight experiments²⁴ appear to show appreciable amounts of energy loss through Rayleigh phonons at $\Theta_i = 65^\circ$ and $k_i \approx 11 \text{ \AA}^{-1}$, where resonances are important.

(v) It is clear that there is in certain cases a very narrow (0.05°) resonant structure (Fig. 3) that is beyond experimental resolution. This happens for high bound states having oscillating extended wave functions (almost continuum states), in agreement with other calculations. We see no evidence of resonances with quasi-bound one-dimensional states, i.e., resonances above the continuum threshold.

(vi) All the calculations reported here are well convergent, yielding good unitarity (within 1%) and what is more important the relations required by symmetry [e.g., the equality of $(\bar{1},1)$ and $(\bar{1},\bar{1})$ at $\phi_i=0$ for varying Θ_i] are also satisfied to the third digit. The convergence of the computation can also be seen from the coherence in the calculated points displayed in the figures. We think that calculated points should be reported in order to know how well the structure is resolved.

Discussions of the matrix elements and magnitude of the splittings existing in the He-LiF(001) band structure have not been presented because

the HCSW model does not give directly the values of the effective matrix elements in the interaction. Qualitatively, one should find results similar to those obtained for other potentials^{18,19} when the bound-state-continuum interaction is neglected, but a more careful treatment incorporating width and shifting of the zero-order bands should be done in this case. In particular, the band structure for a HCSW may be an interesting problem to study because of the remarkable agreement obtained with the experimental scattering data.

ACKNOWLEDGMENTS

We are indebted to Professor D. R. Frankl and co-workers as well as to Professor M. L. Cole for discussions of their work, sometimes in advance of publication. Also one of us (N. G.) is indebted to Center of Advanced studies of the University of Virginia for support. This work has been supported in part by NSF Grant No. DMR-76-17375 and by the National Research Council of Canada under Grant No. A6282.

*Permanent address: Departamento de Física Fundamental, Universidad Autónoma de Madrid, Canto Blanco, Madrid, Spain.

†Permanent address: Department of Applied Math, University of Waterloo, Waterloo, Canada N2L 3G1. Present address: Department of Physics, University of Queensland, St. Lucia, Queensland, Australia 4067.

¹For a recent review, see F. O. Goodman, *CRC Crit. Rev. Solid State Mater. Sci.* **7**, 33 (1977).

²G. Boato, P. Cantini, and L. Mattera, *Surf. Sci.* **55**, 141 (1976).

³U. Garibaldi, A. C. Levi, R. Spadacini, and G. E. Tommei, *Surf. Sci.* **48**, 649 (1975).

⁴N. Garcia, J. Ibanez, J. Solana, and N. Cabrera, *Surf. Sci.* **60**, 385 (1976); *Solid State Commun.* **20**, 1159 (1976).

⁵N. Garcia, *Phys. Rev. Lett.* **37**, 912 (1976); *J. Chem. Phys.* **67**, 897 (1977); K. McCann and V. Celli, *Surf. Sci.* **61**, 10 (1976).

⁶H. U. Finzel, H. Frank, H. Hoinkes, M. Luschka, H. Nahr, W. Wilsch, and H. Wonka, *Surf. Sci.* **49**, 577 (1975).

⁷H. Hoinkes, L. Greiner, and H. Wilsch, in *Proceedings of the Seventh International Vacuum Congress and Third International Conference on Solid Surfaces, Vienna, 1977*, edited by R. Dobrozemsky *et al.* (Berger and Söhne, Vienna, 1977), p. 1349.

⁸J. A. Meyers and D. R. Frankl, *Surf. Sci.* **51**, 61 (1975).

⁹G. Derry, D. Wesner, S. V. Krishnaswamy, and D. R. Frankl, *Surf. Sci.* **74**, 245 (1978); D. R. Frankl, D. Wesner, S. V. Krishnaswamy, G. Derry, and

T. O'Gorman, *Phys. Rev. Lett.* **41**, 60 (1978).

¹⁰I. E. Dzyaloshinskii, I. M. Lifshitz, and L. P. Pitaevskii, *Adv. Phys.* **10**, 165 (1961); C. Mavroyannis, *Mol. Phys.* **7**, 593 (1963); T. H. Boyer, *Phys. Rev.* **180**, 19 (1969).

¹¹M. W. Cole and T. T. Tsong, *Surf. Sci.* **69**, 325 (1977); C. Schwartz, M. W. Cole, and J. Pliva, *ibid.* **75**, 1 (1978).

¹²N. Garcia, F. O. Goodman, V. Celli, and N. R. Hill *Phys. Rev. B* (to be published).

¹³C. E. Harvie and J. H. Weare, *Phys. Rev. Lett.* **40**, 187 (1978).

¹⁴N. Garcia and N. Cabrera, in Ref. 7, p. 379; *Phys. Rev. B* **18**, 576 (1978).

¹⁵A. Marvin and F. Toigo, *Solid State Commun.* **27**, 233 (1978).

¹⁶N. R. Hill and V. Celli, *Phys. Rev. B* **17**, 2478 (1978).

¹⁷H. Chow and E. D. Thompson, *Surf. Sci.* **54**, 269 (1976); N. Garcia, *J. Chem. Phys.* **65**, 2824 (1976).

¹⁸H. Chow and E. D. Thompson, *Surf. Sci.* **59**, 225 (1976).

¹⁹J. Garcia Sanz and N. Garcia, *Surf. Sci.* **79**, 125 (1979).

²⁰The values of these parameters are those that fit better the experimental data (Ref. 2) for $k_z = 11 \text{ \AA}^{-1}$ without considering the attractive well (see Ref. 5).

²¹H. Frank, H. Hoinkes, and W. Wilsch, *Surf. Sci.* **63**, 121 (1977).

²²M. P. Liva and D. R. Frankl, *Surf. Sci.* **59**, 643 (1976).

²³B. Wood, B. F. Mason, and B. R. Williams, *J. Chem. Phys.* **61**, 1435 (1974).

²⁴J. M. Horne and D. R. Miller, *Phys. Rev. Lett.* **41**, 511 (1978).